Phase Relations of the $CaO-SiO_2-Nd_2O_3$ System and the Implication for Rare Earths Recycling

THU HOAI LE, ANNELIES MALFLIET, BART BLANPAIN, and MUXING GUO

$CaO-SiO_2-Nd_2O_3$ slags were equilibrated at 1773 K and 1873 K (1500 °C and 1600 °C) for 24 hours in Ar, and quenched in water to determine the operative phase relations. The composition and crystallinity of the phases in equilibrium were determined by EPMA-WDS and EBSD, respectively. Based on these analyses, the liquid stability region was accurately determined, and a large part of the isothermal section of the phase diagram was constructed. Data resulting from this work can be used to generate a thermodynamic database for rare-earth oxide-containing systems and to support further investigation on separation of rare earths from metallurgical slags or other residues through high-temperature processing.

DOI: 10.1007/s11663-016-0634-9

I. INTRODUCTION

SUSTAINABLE processing of materials is an issue of strong interest around the world and recycling is a major part of this. Rare earth elements (REEs) are some of the most important elements which need to be recovered.[1–3] Recycling is needed to not only secure the supply of REEs for the many technological and other applications in which they are used, it also minimizes the environmental impact related to the extraction of REEs from natural resources, and is one of the solutions proposed to overcome the REE balance problem.[1–6]

A waste stream which contains a rather high content of the critical rare earths, such as Dy, Nd, and Pr, is waste electronics and electrical equipment (WEEE). For its recycling, the emphasis is placed on the three major applications of rare earths: nickel-metal hydride batteries (NiMH), permanent magnets, and lamp phosphors. The price of the rare earths is an important factor in determining the overall cost-effectiveness of recycling. Even during periods of very high prices, their commercial recycling rate for End-of-Life (EoL) products is still very low (below 1 pct in a report of the Working group on the Global Metal Flows for the International Resource Panel/United Nations Environment Program, 2011). The latter is because of the many difficulties in the collection, dismantling, separation, and processing of the REE-containing EoL products. Besides in EoL products, REE can be found in residues from industrial processes, which are high-volume waste streams but contain in general low concentrations of REEs. The possibilities of recycling rare earths from such residues are also still limited according to Binnemans *et al.*[1,2]

Hydrometallurgy is traditionally the main route for the recovery of rare earths, but it requires a large amount of chemicals. A combination with pyrometallurgy, therefore, has been considered as an alternative route with a potentially lower environmental and economic impact.[1,2] In pyrometallurgical processes, rare earth elements, which have high affinity to oxygen, are concentrated in the slag phase. In the recycling of nickel-metal hydride batteries, Muller and Friedrich used $CaO-SiO_2-CaF_2$ to absorb nearly 100 pct of the rare earths and generate 50 to 60 wt pct rare-earth-containing slag.[7] Later, Tang *et al.*[8] performed slagging treatment experiments at 1700 K (1427 °C) in which they used calcium silicate slag to collect almost all rare earths in the slag and to recover nickel cobalt alloys. The slag consisted of 46 wt pct rare earth oxides. Elwert *et al.*[9] reported that with an addition of P_2O_5 to the $Al_2O_3-CaO-MgO-SiO_2$ system for the recycling of NdFeB magnets, 57 wt pct rare-earth oxide-containing phase (britholite-like silicophosphate) was formed. A further challenge for metallurgists is to find an efficient extraction process to recover the rare earths, as it appears difficult to separate the rare earths from the slags.

In order to enhance the rare earths recycling efficiency through pyrometallurgical processing, fundamental understanding of the rare earths distribution in the slag is of significant importance. Such knowledge allows selecting suitable fluxes and other process parameters, such as temperature and atmosphere. However, the availability of thermodynamic data for rare earth oxide systems, which is necessary for rare earths recovery through pyrometallurgical processes,[7–9] is insufficient even for the Neodymium-containing $CaO-SiO_2$ slag system. The $CaO-SiO_2$ and $SiO_2-Nd_2O_3$ binary subsystems were investigated elsewhere.[10,11] Although several phase diagrams of the $CaO-RE_xO_y$ family (RE = La, Dy, Y, Gd, Pr) have been studied for decades,[12] the binary $CaO-Nd_2O_3$ has only been studied to some extent recently.[13] There are only few studies on solid state

THU HOAI LE, Ph.D Student, ANNELIES MALFLIET, Postdoctoral Researcher, BART BLANPAIN, Professor, and MUXING GUO, Senior Research Expert, are with the Department of Materials Engineering, KU Leuven, Kasteelpark Arenberg 44 Bus 2450, 3001 Heverlee, Leuven, Belgium. Contact e-mail: thuhoai.le@mtm.kuleuven.be

Manuscript submitted December 1, 2015.
Article published online March 16, 2016.

equilibrium of $CaO\text{-}Nd_2O_3\text{-}SiO_2$ ternary system reported in late 60s and 70s,[14,15] neither data nor information of solid solution solubility or the liquidus have been found.

This work, therefore, will experimentally investigate the phase relations of $CaO\text{-}SiO_2\text{-}Nd_2O_3$ system at 1773 K and 1873 K (1500 °C and 1600 °C) under inert argon atmosphere using a quenching technique followed by compositional analysis of equilibrated samples. Based on the results, the rare earth recycling feasibility in $CaO\text{-}Nd_2O_3\text{-}SiO_2$ is discussed.

II. EXPERIMENTAL

A. *Materials and Crucible*

To avoid sample contamination, high-purity fine powders were used as starting materials. Samples were prepared from CaO powder (obtained by calcination of $CaCO_3$, 99.99 pct, Chempur, CAS No.: 471-34-1), SiO_2 (99.9 pct, Merck Millipore, CAS No.: 14808-60-7), and Nd_2O_3 (99.99 pct, Chempur, CAS No.: 1313-97-9).

As the crucible material, Pt-20 pctRh was selected based on the used slag chemistry and the desired cooling rate. Considering the large number of samples and the aim to prevent high wetting of the slag with the container material, closed shallow-bottomed envelopes were designed by folding 0.1-mm-thick Pt-20 pctRh foil (Figure 1). With this design, one experiment can carry tens of samples. The foils can be reused after cleaning with HF.

III. EXPERIMENTAL PROCEDURE

The oxide powders were weighed using an analytical balance with 0.01 mg accuracy and mixed according to Tables I and II. The CaO/SiO_2 weight ratios of the samples were from 0.09 to 8.4 and from 0.04 to 18 at 1773 K and 1873 K (1500 °C and 1600 °C), respectively. 20 mg of the powder mixture was put in the closed shallow-bottomed envelopes. Then the envelopes were placed in a protection alumina crucible which was positioned with a Pt-20 pctRh/Mo wire in the hot zone of a vertical tube furnace with $MoSi_2$ heating elements. The furnace temperature was monitored within 1 K (1 °C) by a type B (Pt-6 pctRh) thermocouple. The hot zone was measured to be within 2 cm with 1 K (1 °C) in error. The samples were then heated in the furnace under Argon atmosphere (flow rate 400 cm^3/min), and kept at the desired temperature [1773 K or 1873 K (1500 °C or 1600 °C)] for 24 hours to attain equilibrium, before quenching in cold water. It is assumed that a fast cooling rate was achieved due to the small size of the slag sample and its container. The equilibration time was determined by comparing the amount of Nd_2O_3 dissolved in the glass phase after different equilibration times (6, 12, 24, and 72 hours) under different heating routes for rare-earth-rich and silica-rich samples. It was concluded that 24 hours dwelling time was sufficient for the liquid-state equilibrium. The schematic diagram of the experimental apparatus is shown in Figure 2.

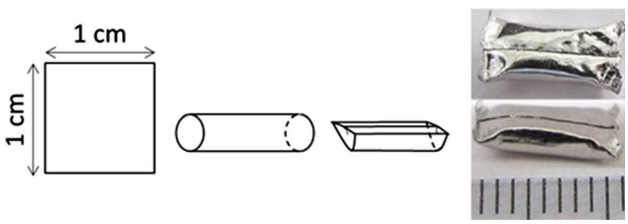

Fig. 1—Pt-20 pctRh closed shallow-bottomed envelope.

A. *Compositional Analysis and Phase Identification*

The quenched samples were mounted in resin, grinded and polished. For microstructure and phase composition analysis, the samples were carbon coated, and analyzed by electron probe micro-analysis (EPMA, JEOL JXA-8530F) using standardized wavelength dispersive spectroscopy (WDS) and operated at 15 kV to 15 nA. A 16.9wt pct CaO-12.1wt pctAl_2O_3-54.3wt pctSiO_2-16.7wt pctNd_2O_3 glass was used as standard. The average accuracy the of EPMA measurements on the main elements is ±1 wt pct. The content of possible contaminations from Mo, Rh and Pt, were measured to be less than 0.1 wt pct. The presence of liquid phase in the samples was verified by a Field Emission Gun Electron Microscope FEI-Nova Nanosem 450 using electron backscatter diffraction (EBSD) in low vacuum at 20 kV. For some loosely packed samples after quenching, XRD on powders was used to examine and confirm the presence of phases as determined by EPMA.

IV. RESULTS AND DISCUSSION

A. *Phases Present at 1773 K and 1873 K (1500 °C and 1600 °C)*

Microstructural examination of the obtained samples indicates the presence of SiO_2, Nd_2O_3, $Nd_2Si_2O_7$, $Nd_{9.33}(SiO_4)_6O_2$, $CaNd_2O_4$, calcium neodymium silicate oxide $Ca_{2+x}Nd_{8-x}(SiO_4)_6O_{2-0.5x}$ (TC), the solid solutions of CaO(Nd2O3), Nd2O3(CaO), $CS(Nd_2O_3)$, $C_2S(Nd_2O_3)$, and $C_3S(Nd_2O_3)$, and the liquid slag phase. Examples of typical microstructures for the quenched samples are shown in Figures 3 and 4. The irregularly shaped SiO_2 and Nd_2O_3 (Figures 3(d) through (h)) in the samples are believed to be undissolved initial SiO_2 and Nd_2O_3 particles, resulting from saturation of the system in these compounds. The extra experiments at 72 hours dwelling time confirmed these Nd_2O_3-rich and SiO_2-rich samples reached the equilibrium. The calcium neodymium silicate oxide $Ca_{2+x}Nd_{8-x}(SiO_4)_6O_{2-0.5x}$ forms multi-faceted crystals and is in equilibrium with liquid slag (Figure 3(c)) and/or other solid phases, such as SiO_2 (Figure 3(f)) and $C_2S(Nd_2O_3)$ (Figure 3(i)). It should be noted that the applied high cooling rate during quenching results in the preservation of the high-temperature solid phases and transformation of the liquid phase into a glass phase without crystal precipitation at room temperature. From the shape of the

Table I. Experiment Data for the System CaO-SiO_2-Nd_2O_3 at 1773 K (1500 °C)

	Initial Composition (Weight Percentage)				Final Composition (Weight Percentage)			
Sample	SiO_2	Nd_2O_3	CaO	Phase	SiO_2	Nd_2O_3	CaO	x
$Ca_{2+x}Nd_{8-x}(SiO_4)_6O_{2-0.5x}$ + liquid								
1	35	35	30	$Ca_{2+x}Nd_{8-x}(SiO_4)_6O_{2-0.5x}$	21	70.1	8.9	0.7
				liquid	42.6	20.4	37	
2	35	45	20	$Ca_{2+x}Nd_{8-x}(SiO_4)_6O_{2-0.5x}$	19.4	74.3	6.3	0.1
				liquid	46.9	29.4	23.7	
3	35	45	20	$Ca_{2+x}Nd_{8-x}(SiO_4)_6O_{2-0.5x}$	18.9	74.3	6.8	0.3
				liquid	44.3	26.4	29.3	
4	35	53	12	$Ca_{2+x}Nd_{8-x}(SiO_4)_6O_{2-0.5x}$	19.2	74.8	6	0.0
				liquid	50.3	33.4	16.3	
5	45	40	15	$Ca_{2+x}Nd_{8-x}(SiO_4)_6O_{2-0.5x}$	19.1	74.5	6.4	0.2
				liquid	50.2	32.7	17.1	
6	40	30	30	$Ca_{2+x}Nd_{8-x}(SiO_4)_6O_{2-0.5x}$	20.2	72.1	7.7	0.5
				liquid	43.9	22.3	33.8	
SiO_2 + liquid								
7	70	12	18	liquid	56.2	19.3	24.5	
				SiO_2	99.9	0.1	0	
8	65	23	12	liquid	99.8	0.2	0	
				SiO_2	49.5	32.2	18.3	
9	78	2	20	SiO_2	99.5	0.1	0.4	
				liquid	63.9	3.9	32.2	
10	79	2	19	liquid	64.5	3.3	32.2	
				SiO_2	99.8	0	0.2	
11	82	3	15	liquid	66.5	3.3	30.2	
				SiO_2	99.8	0	0.2	
12	84	2	14	liquid	67.8	1.8	30.4	
				SiO_2	99.9	0	0.1	
13	65	10	25	liquid	52.9	32.8	14.3	
				SiO_2	99.7	0.2	0.1	
	70	10	20	SiO_2	99.7	0.2	0.1	
				liquid	60.1	15.1	24.8	
$C_2S(Nd_2O_3)$ + liquid								
14	38	4	58	$C_2S(Nd_2O_3)$	33.5	7	59.5	
				liquid	44.5	2.9	52.6	
16	38	9	53	liquid	49.5	8.7	41.8	
				$C_2S(Nd_2O_3)$	32.3	11.1	56.6	
17	38	10	52	liquid	47.8	10.5	41.7	
				$C_2S(Nd_2O_3)$	33.1	10.4	56.5	
CS + liquid								
18	51	1	48	liquid	58.1	3.7	38.2	
				CS	50.6	0.3	49.1	
19	51	1.5	47.5	liquid	58.6	3	38.4	
				CS	50.6	0.1	49.3	
20	51	2	47	liquid	59.6	3.6	36.8	
				CS	50.9	0.2	48.9	
21	46	3	51	CS	50.7	0.7	48.6	
				liquid	52.6	9.8	37.6	
22	45	2	53	liquid	56.6	5.9	37.5	
				CS	50.6	0.5	48.9	
23	45	3	52	liquid	55.8	9.7	34.5	
				CS	50.7	0.5	48.8	
24	44	2	54	liquid	57.6	4.6	37.8	
				CS	50.5	0.2	49.3	
SiO_2 + Nd_2O_3 + $Ca_{2+x}Nd_{8-x}(SiO_4)_6O_{2-0.5x}$								
25	22	75	3	SiO_2	99.7	0.3	0	
				Nd_2O_3	0	99.3	0.7	
				$Ca_{2+x}Nd_{8-x}(SiO_4)_6O_{2-0.5x}$	20.1	72.7	7.2	
$Ca_{2+x}Nd_{8-x}(SiO_4)_6O_{2-0.5x}$ + SiO_2 + Liquid								
26	47	45		$Ca_{2+x}Nd_{8-x}(SiO_4)_6O_{2-0.5x}$	19.5	74.4	6.1	0.0
			8					
				liquid	50	33.2	16.8	

Table I. Continued

Sample	Initial Composition (Weight Percentage)			Phase	Final Composition (Weight Percentage)			x
	SiO_2	Nd_2O_3	CaO		SiO_2	Nd_2O_3	CaO	
				SiO_2	99.7	0.3	0	
27	50	40	10	liquid	50.6	32.7	16.7	
				$Ca_{2+x}Nd_{8-x}(SiO_4)_6O_{2-0.5x}$	19.6	74.5	5.9	0.1
				SiO_2	99.7	0.3	0	
$Ca_{2+x}Nd_{8-x}(SiO_4)_6O_{2-0.5x}$ + Nd_2O_3 + $C2S(Nd_2O_3)$								
28	20	60	20	Nd_2O_3	0.4	98.6	1	
				$Ca_{2+x}Nd_{8-x}(SiO_4)_6O_{2-0.5x}$	19.5	74	6.5	0.1
				$C_2S(Nd_2O_3)$	32.2	14.5	53.3	
29	15	70	15	Nd_2O_3	0.4	98.6	1	
				$Ca_{2+x}Nd_{8-x}(SiO_4)_6O_{2-0.5x}$	19.5	74	6.5	0.1
				$C_2S(Nd_2O_3)$	32.2	14.5	53.3	
30	22	50	28	$Ca_{2+x}Nd_{8-x}(SiO_4)_6O_{2-0.5x}$	20.4	72.6	7	0.2
				$C_2S(Nd_2O_3)$	32.3	13.9	53.8	
				Nd_2O_3	0.4	98.7	0.9	
$Ca_{2+x}Nd_{8-x}(SiO_4)_6O_{2-0.5x}$ + liquid + $C2S(Nd_2O_3)$								
31	22	38	40	$C_2S(Nd_2O_3)$	31.9	22.1	46	
				liquid	41.4	16.9	41.7	
				$Ca_{2+x}Nd_{8-x}(SiO_4)_6O_{2-0.5x}$	20.7	70.4	8.9	0.8
$C_2S(Nd_2O_3)$ + $C_3S(Nd_2O_3)$ + Nd_2O_3								
32	20	20	60	Nd_2O_3	0	97.6	2.4	
				$C_3S(Nd_2O_3)$	25	10	65	
				$C_2S(Nd_2O_3)$	33.1	8.2	58.7	

Table II. Experiment Data for the System CaO-SiO_2-Nd_2O_3 at 1873 K (1600 °C)

Sample	Initial Composition (Weight Percentage)			Phase	Final Composition (Weight Percentage)			x
	SiO_2	Nd_2O_3	CaO		SiO_2	Nd_2O_3	CaO	
$Ca_{2+x}Nd_{8-x}(SiO_4)_6O_{2-0.5x}$ + liquid								
1	37.5	37.5	25	$Ca_{2+x}Nd_{8-x}(SiO_4)_6O_{2-0.5x}$	21.8	70.7	7.5	0.2
				liquid	44.5	29.1	26.4	
2	33.3	33.4	33.3	liquid	41.1	20.3	38.6	
				$Ca_{2+x}Nd_{8-x}(SiO_4)_6O_{2-0.5x}$	22.4	68.2	9.4	0.7
3	30	40	20	liquid	41.9	22.9	35.2	
				$Ca_{2+x}Nd_{8-x}(SiO_4)_6O_{2-0.5x}$	20.4	71.8	7.8	0.5
SiO_2 + liquid								
4	70	20	10	liquid	52.7	29.9	17.4	
				SiO_2	99.7	0.2	0.1	
5	60	20	20	SiO_2	99.8	0.1	0.1	
				liquid	55.4	22.2	22.4	
6	70	10	20	SiO_2	99.7	0.2	0.1	
				liquid	60.1	15.1	24.8	
7	75	2	23	liquid	63.5	2.3	34.2	
				SiO_2	99.9	0	0.1	
8	31	5	64	SiO_2	99.9	0	0.1	
				liquid	65.2	3.9	30.9	
$C_2S(Nd_2O_3)$ + liquid								
9	27	8	65	liquid	43.6	3.7	52.7	
				$C_2S(Nd_2O_3)$	33.6	7	59.4	
10	48	5	47	liquid	43.2	5.4	51.4	
				$C_2S(Nd_2O_3)$	33	8.7	58.3	
11	37	2	61	$C_2S(Nd_2O_3)$	34.1	2.5	63.4	
				liquid	43.6	1	55.4	
12	37	8	55	$C_2S(Nd_2O_3)$	32.6	10.3	57.1	
				liquid	43.5	6.4	50.1	
13	37	15	48	liquid	41.7	12.8	45.5	

Table II. Continued

Sample	Initial Composition (Weight Percentage)			Phase	Final Composition (Weight Percentage)			
	SiO_2	Nd_2O_3	CaO		SiO_2	Nd_2O_3	CaO	x
				$C_2S(Nd_2O_3)$	31.6	17.3	51.1	
14	37	18	45	$C_2S(Nd_2O_3)$	31.3	19.3	49.4	
				liquid	41.1	15.1	43.8	
$Ca_{2+x}Nd_{8-x}(SiO_4)_6O_{2-0.5x}$ + $C_2S(Nd_2O_3)$ + liquid								
15	37	25	38	liquid	43.4	14.2	42.4	
				$Ca_{2+x}Nd_{8-x}(SiO_4)_6O_{2-0.5x}$	19.9	72.1	8.0	0.6
				$C_2S(Nd_2O_3)$	30.9	23.3	45.8	
$Ca_{2+x}Nd_{8-x}(SiO_4)_6O_{2-0.5x}$ + SiO_2 + Nd_2O_3								
16	12	85	3	$Ca_{2+x}Nd_{8-x}(SiO_4)_6O_{2-0.5x}$	19.5	74.5	6	0
				SiO_2	97.53	1.96	0.51	
				Nd_2O_3	0	99.8	0.2	
17	32	65	3	SiO_2	99.7	0.3	0	
				Nd_2O_3	0	99.3	0.7	
				$Ca_{2+x}Nd_{8-x}(SiO_4)_6O_{2-0.5x}$	20.1	72.7	7.2	0.3
$Ca_{2+x}Nd_{8-x}(SiO_4)_6O_{2-0.5x}$ + SiO_2 + liquid								
18	34	60	6	liquid	44.8	44.8	10.4	
				SiO_2	99.6	0.3	0.1	
				$Ca_{2+x}Nd_{8-x}(SiO_4)_6O_{2-0.5x}$	21.3	72.4	6.3	0.1
19	50	40	10	$Ca_{2+x}Nd_{8-x}(SiO_4)_6O_{2-0.5x}$	21.3	71.5	7.2	0.2
				SiO_2	99.8	0.2	0	
				liquid	45.1	43.9	11	
$Ca_{2+x}Nd_{8-x}(SiO_4)_6O_{2-0.5x}$ + $C_2S(Nd_2O_3)$ + Nd_2O_3								
20	15	70	15	$Ca_{2+x}Nd_{8-x}(SiO_4)_6O_{2-0.5x}$	20.3	72.9	6.8	0.2
				$C_2S(Nd_2O_3)$	32.9	16.2	50.9	
				Nd_2O_3	0.4	96.5	3.1	
21	14	80	6	$Ca_{2+x}Nd_{8-x}(SiO_4)_6O_{2-0.5x}$	20.2	73	6.8	0.2
				$C_2S(Nd_2O_3)$	31.6	16.6	51.8	
				Nd_2O_3	0.1	98.4	1.5	
C2S(Nd_2O_3) + C3S(Nd_2O_3) + CaO								
22	5	5	90	$C_2S(Nd_2O_3)$	33.1	8.3	58.6	
				$C_3S(Nd_2O_3)$	24.9	9.1	66	
				CaO	0	0.1	99.9	
23	22	3	75	$C_2S(Nd_2O_3)$	34	3	63	
				$C_3S(Nd_2O_3)$	26.1	3.2	70.7	
				CaO	0.5	0.1	99.4	
$C_2S(Nd_2O_3)$ + $C_3S(Nd_2O_3)$ + Nd_2O_3								
24	20	20	60	Nd_2O_3	0.1	97	2.9	
				$C_3S(Nd_2O_3)$	24.9	11	65.3	
				$C_2S(Nd_2O_3)$	32.1	9	58.9	

phase boundaries in a 2D image, it is often possible to distinguish the liquid and solid phases, but sometimes it is not clear. For example, the spherically appearing particles, as shown in Figures 3(b) and (i), can be liquid droplets or the cross sections of dendritic arms. If the composition of these particles falls within a region where the solid solubility of the phases or the extent of the liquid region is unknown, compositional analysis will not provide an answer to the question whether this phase was liquid or solid at high temperature. Therefore, EBSD was used whenever this ambiguity appeared, to clarify the crystalline or amorphous nature of the phases by recording the Kikuchi patterns, as illustrated in Figure 5. Hence, with the combination of EPMA and EBSD, solid solution phases of C_2S (Nd_2O_3) were detected and their solubility data were determined.

B. *Phase Equilibria and Construction of the CaO-Nd_2O_3-SiO_2 Isothermal Sections at 1773 K and 1873 K (1500 °C and 1600 °C)*

1. *Binary systems*

According to literature,[10,11] for the involved binaries Nd_2O_3-SiO_2 and CaO-SiO_2 at 1773 K and 1873 K (1500 °C and 1600 °C), three incongruently melting compounds, namely C_3S, Nd_2SiO_5, and $Nd_2Si_2O_7$, and three congruently melting compounds, namely $Nd_{9.33}(SiO_4)_6O_2$, C_2S and CS, exist. This study confirmed the presence of these binary Nd_2O_3-SiO_2 compounds as seen in Figure 4. In the present study, solid solutions of less than 4 wt pct of CaO in Nd_2O_3 and less than 12 wt pct of Nd_2O_3 in CaO of the CaO-Nd_2O_3 system were found at both 1773 K and 1873 K (1500 °C and 1600 °C).

2. *Ternary system*

For the ternary CaO-Nd_2O_3-SiO_2 system, the existing phases and their compositions as determined in this study are given in Tables I and II. For each sample, ten composition measurements were done within the selected phase at various locations and the average value is reported. The data in Tables I and II are organized and presented such that all measurements relating to a particular primary phase field or a combination of phases are grouped together. Samples that consist of at least 2 homogeneous phases in equilibrium with each other are used to determine the phase equilibria. From the phase equilibria, the isothermal sections at 1773 K and 1873 K (1500 °C and 1600

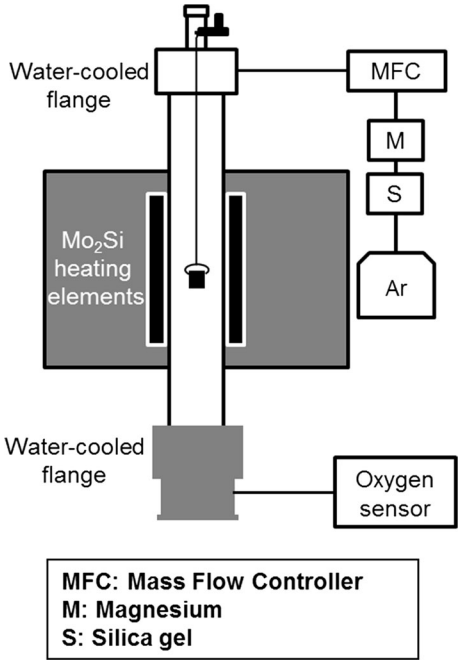

Fig. 2—A schematic illustration of the experimental setup.

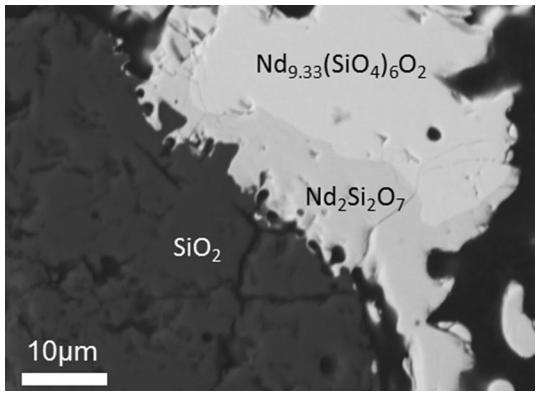

Fig. 4—BSE image (*a*, *b*) phases present in the binary SiO_2-Nd_2O_3 and CaO-Nd_2O_3 system, respectively.

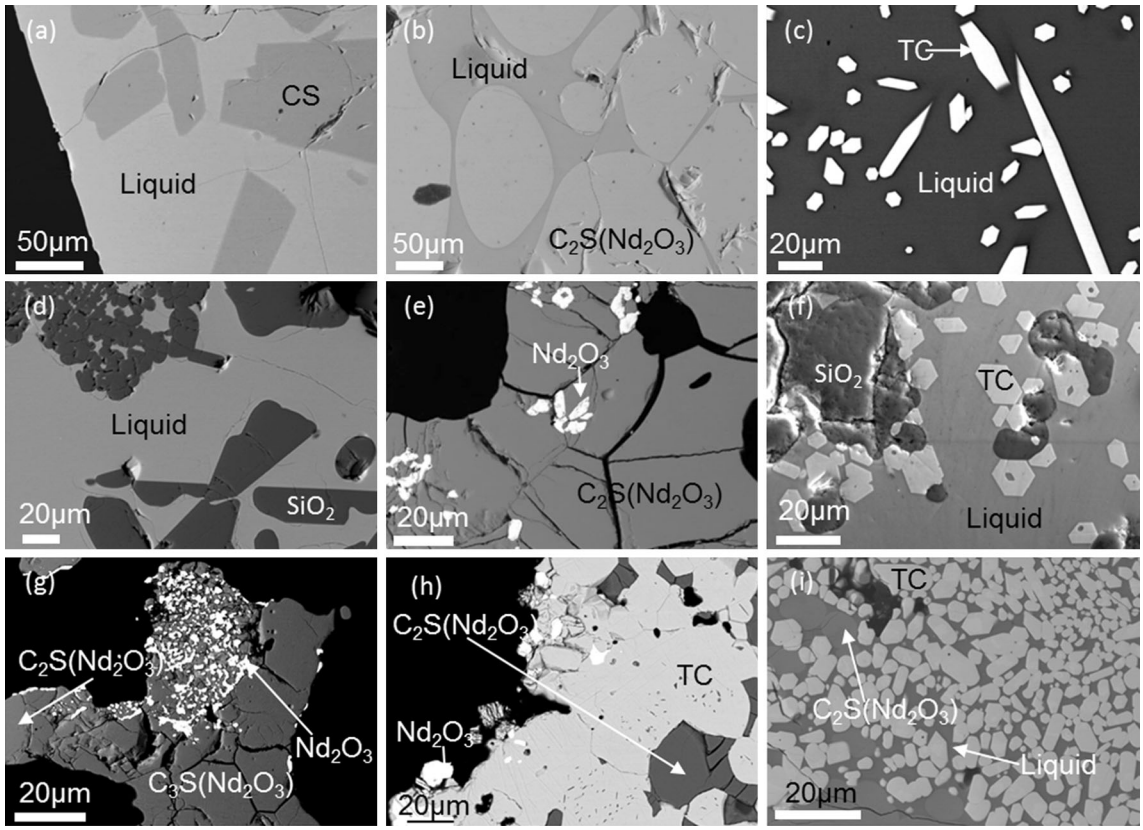

Fig. 3—BSE image (*a*) through (*d*) one solid phase in equilibrium with one liquid phase, (*e*) $C_2S(Nd_2O_3)$ in equilibrium with Nd_2O_3, (*g*, *h*) three solid phases in equilibrium, (*f*, *i*) two solid phases in equilibrium with one liquid phase.

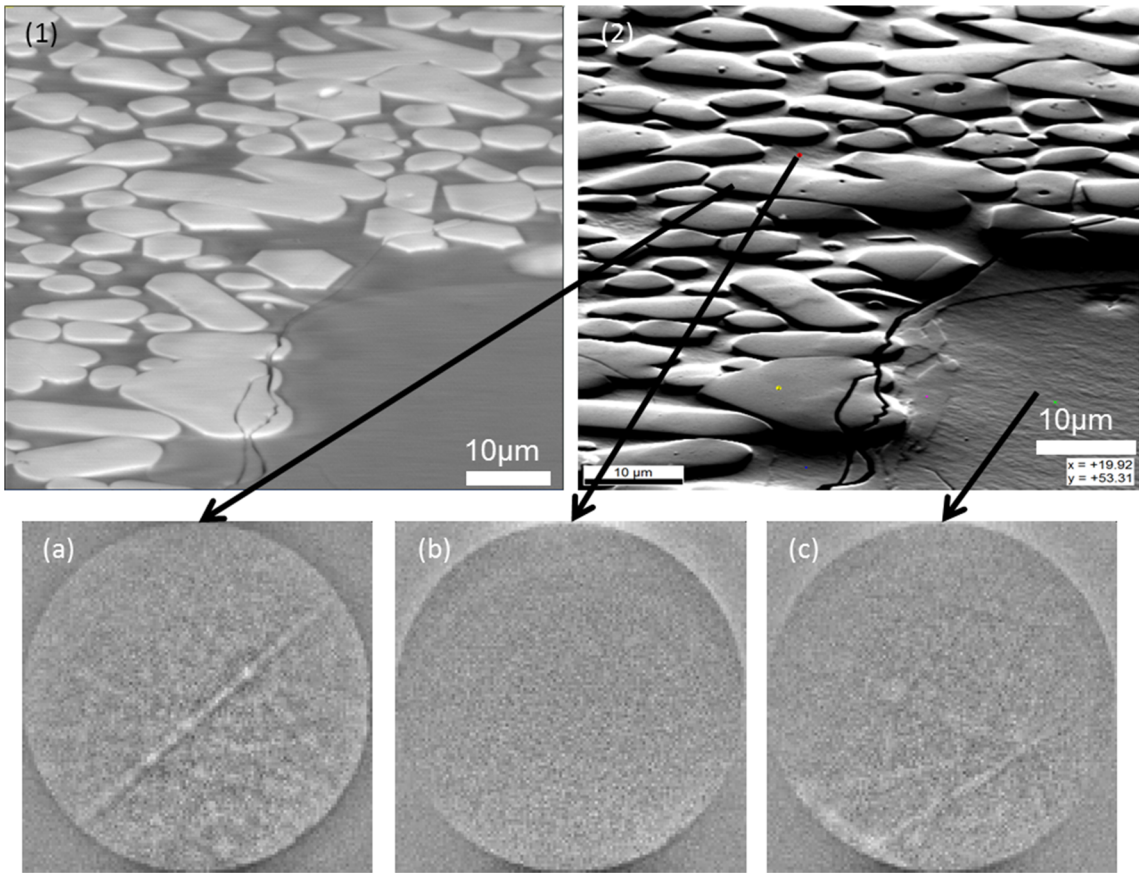

Fig. 5—EBSD images (*1*) BSE image, (*2*) SE image; Kikuchi pattern of (*a*) liquid phase, (*b*) calcium neodymium silicate oxide $Ca_{2+x}Nd_{8-x}(SiO_4)_6O_{2-0.5x}$ solid phase, and (*c*) $C_2S(Nd_2O_3)$ solid solution phase.

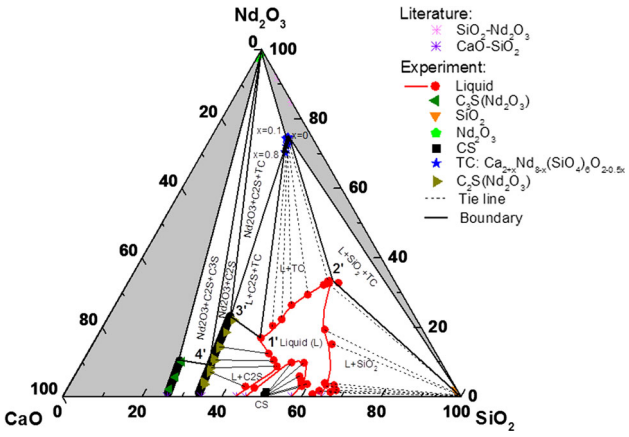

Fig. 6—Isothermal section of $CaO\text{-}SiO_2\text{-}Nd_2O_3$ phase diagram and tie-lines at 1773 K (1500 °C). The phase relations in the $CaO\text{-}C_3S\text{-}Nd_2O_3$ triangle are not determined in this study.

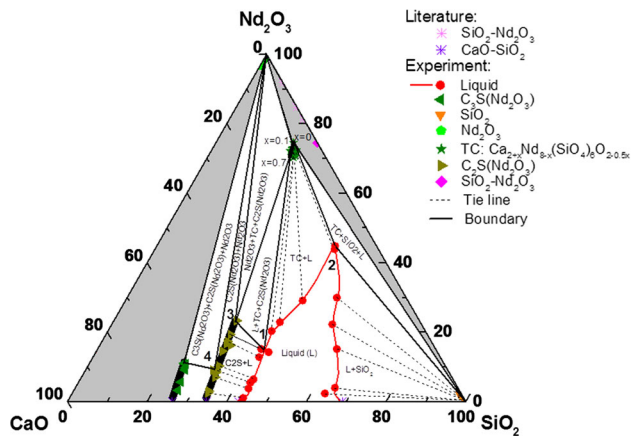

Fig. 7—Isothermal section of $CaO\text{-}SiO_2\text{-}Nd_2O_3$ phase diagram and tie-lines at 1873 K (1600 °C). The phase relations in the $CaO\text{-}C_3S\text{-}Nd_2O_3$ triangle are not determined in this study.

°C) of the $Ca_3SiO_5(C_3S)\text{-}SiO_2\text{-}Nd_2O_3$ region in the $CaO\text{-}SiO_2\text{-}Nd_2O_3$ phase diagram are constructed by applying Rhines' ten empirical rules and the boundary theory[16] (Figures 6 and 7). For compositions within the $CaO\text{-}Nd_2O_3\text{-}C_3S$ and $Nd_2O_3\text{-}SiO_2\text{-}TC$ triangles, the samples obtained after quenching, however, were in the form of loosely packed powders. Therefore, only the $Ca_3SiO_5(C3S)\text{-}SiO_2\text{-}Nd_2O_3$ pseudoternary system is considered in the construction of Figures 6 and 7.

3. *Solid solutions*

The solubility limit of Nd_2O_3 in Ca_3SiO_5 (C_3S) and Ca_2SiO_4 (C_2S) increases from 1773 K to 1873 K (1500 °C to 1600 °C), and these values are documented in Table III.

Table III. Solubility Limit Data of Nd_2O_3 in C_2S and C_3S

	Weight Percentage Nd_2O_3	
Temperature	C2S	C3S
1773 K (1500 °C)	22.1	10
1873 K (1600 °C)	23.3	11

By using XRD powder, Jantzen and Glasser[15] reported that the substitutions of RE silicate into C_2S, C_3S produced β-C_2S and R-C_3S solid solutions, respectively. Unfortunately, the solubility as well as liquid phase compositions were not measured in their study. The existence of the $C_3S(Nd_2O_3)$-$C_2S(Nd_2O_3)$-Nd_2O_3, $C_2S(Nd_2O_3)$-TC-Nd_2O_3 three-phase regions was also observed in their work.

The ternary compound was reported to have the formula of $Ca_{2+x}Nd_{8-x}(SiO_4)_6O_{2-0.5x}$ and x was suggested to be 0 at 1873 K (1600 °C).[17] In the present work, however, a deviation in composition of the ternary compound was observed for both 1773 K and 1873 K (1500 °C and 1600 °C). The solubility of Ca in $Ca_{2+x}Nd_{8-x}(SiO_4)_6O_{2-0.5x}$ is x = 0–0.8 and 0–0.7 at, respectively, 1773 K and 1873 K (1500 °C and 1600 °C) (Tables I and II). The solubility limits of Ca in $Ca_{2+x}Nd_{8-x}(SiO_4)_6O_{2-0.5x}$ decreases at increasing temperature which is in good agreement with Fahey's suggestion.[17] In another publication,[18] the authors provide more crystallographic data as obtained by XRD single crystal for the ternary compound at 1873 K (1600 °C) in equilibrium with liquid and having x = 0.49.

4. *Liquid region*

In the isothermal sections in Figures 6 and 7, the liquidus is displayed by a red line. At 1873 K (1600 °C), three primary phases exist, namely SiO_2, $C_2S(Nd_2O_3)$ solid solution and the ternary compound $Ca_{2+x}Nd_{8-x}(SiO_4)_6O_{2-0.5x}$. At 1773 K (1500 °C), another primary phase, namely CS, appears. The tie-lines between liquid and CS, C_2S, SiO_2, and $Ca_{2+x}Nd_{8-x}(SiO_4)_6O_{2-0.5x}$ in the two-phase regions are also indicated. The amount of liquid at any point along these tie-lines can be determined by the Lever rule. In Figure 8, the effect of temperature on the liquid region is illustrated in more detail, where the blue and red lines are the liquidus lines at 1873 K and 1773 K (1600 °C and 1500 °C), respectively. As part of the liquidus surface, these liquidus lines show the tendency of the solidification path. The solubility of Nd_2O_3 in the liquid phase decreases with decreasing the temperature and its limit is up to nearly 45 wt pct at 1873 K (1600 °C) and 33 wt pct at 1773 K (1500 °C). When temperature decreases from 1873 K to 1773 K (1600 °C to 1500 °C), points 1 and 2 moved to 1′ and 2′. Those four points are positioned on two eutectic lines which present the equilibrium between liquid and two solid phases. Along the liquidus belonging to the two-phase equilibrium of liquid and $Ca_{2+x}Nd_{8-x}(SiO_4)_6O_{2-0.5x}$, the solubility of Nd_2O_3 in the liquid phase increased with decreasing C/S ratio at both investigated temperatures.

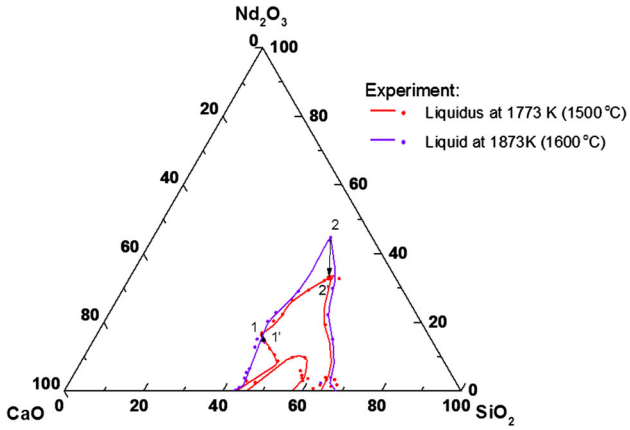

Fig. 8—Temperature dependence of the liquidus in the CaO-SiO_2-Nd_2O_3 system.

C. *Recycling Feasibility*

The isothermal sections in Figures 5 and 6 provide new data on the phase equilibria and slag liquidus in the ternary CaO-Nd_2O_3-SiO_2 system. These isothermal sections not only give instructions to select the composition of an industrial slag but also show the potential of recycling REE through calcium silicate-based slag processing.

The behavior of REE in this slag system is clearly interpreted from these isothermal sections. It provides information regarding the selection of suitable flux materials for rare-earth-containing waste recycling processes from which their slags are considered as the starting secondary raw materials, as an alternative to rare earth ores. The present work shows that there are two regions of interest besides the liquid region: the two-phase region of $Ca_{2+x}Nd_{8-x}(SiO_4)_6O_{2-0.5x}$ in equilibrium with liquid and the two-phase region of CS in equilibrium with liquid. These two-phase regions were quantitatively determined, providing quantitative insight for REEs separation and/or concentration from the REE-containing wastes. In order to enhance the REE recovery and slag recycling potential, a hot stage slag treatment process can be followed. By post-process additions to the high-temperature slag without interfering with the metallurgical process, the slag chemistry is changed; and/or with subsequent variations in the cooling paths, the phases of interest for optimizing the recycling process are produced.

1. *Precipitation of REE-rich solid phase in liquid + $Ca_{2+x}Nd_{8-x}(SiO_4)_6O_{2-0.5x}$ region*

The high rare-earth-containing phase $Ca_{2+x}Nd_{8-x}(SiO_4)_6O_{2-0.5x}$ was found to be stable at high temperature. Because it has a higher density compared to the liquid phase, it will precipitate at the bottom of the container, as it was also observed in our experiments (Figure 9). By separating these $Ca_{2+x}Nd_{8-x}(SiO_4)_6O_{2-0.5x}$ precipitates from the slag, a REE-enriched product is obtained, which can serve as a REE-rich input stream in a next step of the REE recycling process.

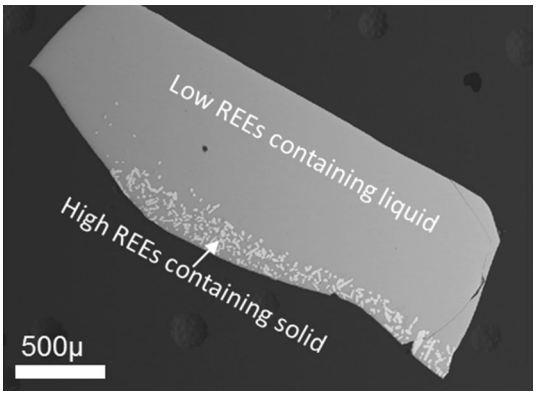

Fig. 9—Precipitation of $Ca_{2+x}Nd_{8-x}(SiO_4)_6O_{2-0.5x}$ phase in the liquid slag.

For industrial practice, however, the viscosity of the molten slag should be studied in advance since the slag viscosity will significantly affect the $Ca_{2+x}Nd_{8-x}(SiO_4)_6O_{2-0.5x}$ precipitate sedimentation (to the container bottom), therefore influencing the separation efficiency. An alternative approach could be to separate the $Ca_{2+x}Nd_{8-x}(SiO_4)_6O_{2-0.5x}$ precipitates by physical mineral processing schemes.

2. *Concentrating of REE in Liquid + CS region*

From Figure 6, it is clear that for slag compositions in the CS primary phase field, a separation between the REE-containing liquid phase and the REE-poor CS compound will occur. With slags containing low rare earths content, a suitable cooling trajectory can enrich the rare earths in the liquid phase and precipitate the CS compound. Thus, the work load for recycling rare earth will be reduced, hence increasing the economic viability of the recycling process.

V. CONCLUSIONS

The isothermal sections in the Ca_3SiO_5-SiO_2-Nd_2O_3 pseudoternary system at 1873 K and 1773 K (1600 °C and 1500 °C) have been constructed by using a quenching technique followed by compositional analysis of equilibrated samples. The combination of EPMA-WDS and Nanosem-EBSD provides crucial evidence for the classification of the amorphous phase and for the determination of solubility data of the solid solutions. The investigated phase relations can be used for optimizing the thermodynamic database and separation of Nd_2O_3 from the slag in future work. Based on the phase relations of CaO-SiO_2-Nd_2O_3 system measured in present work, two possible REE recycling schemes are proposed: (1) precipitation of REE-rich solid phase in Liquid + $Ca_{2+x}Nd_{8-x}(SiO_4)_6O_{2-0.5x}$ region; and (2) concentrating of REE in Liquid + CS region.

ACKNOWLEDGMENTS

The authors acknowledge the support from the Hercules Foundation (Project No. ZW09-09) in the use of the FEG-EPMA and FEI-Nova Nanosem system and from the GOA/13/008 project at the KU Leuven.

REFERENCES

1. K. Binnemans, P.T. Jones, B. Blanpain, T. Van Gerven, Y. Yang, A. Walton, and M. Buchert: *J. Clean. Prod.*, 2013, vol. 51, pp. 1–22.
2. K. Binnemans, P.T. Jones, B. Blanpain, T. Van Gerven, and Y. Pontikes: *J. Clean. Prod.*, 2015, vol. 99, pp. 17–38.
3. S. Chu: *Critical Materials Strategy*, U.S. Department of Energy, December 2011. http://energy.gov/sites/prod/files/DOE_CMS2011_FINAL_Full.pdf.
4. R.J. Weber and D.J. Reisman: *Rare Earth Element: A Review of Production, Processing, Recycling, and Associated Environmental Issues*, U.S. Environmental Protection Agency, August 2012. http://www.epa.gov/superfund/remedytech/tsp/download/2012_spring_meeting/fff_wed/4_weber-rare_earth_minerals.pdf.
5. L.T. Peiro, G.V. Mendez, and R.U. Ayres: *Rare and Critical Metals as By-products and the Implications for Future Supply*, INSEAD Social Innovation Centre, 2011. http://www.insead.edu/facultyresearch/research/doc.cfm?did=48916.
6. T.G. Goonan: *Rare earth elements—End use and recyclability*, U.S. Geological Survey Scientific Investigations Report 5094, 2011. http://pubs.usgs.gov/sir/2011/5094/.
7. T. Müller and B. Friedrich: *J. Power Sources*, 2006, vol. 158 (2), pp. 1498–1509.
8. K. Tang, A. Ciftja, C. van der Eijk, S. Wilson, and G. Tranell: *J. Min. Metall. Sect. B*, 2013, vol. 49, pp. 233–36.
9. T. Elwert, D. Goldmann, T. Schirmer, and K. Strauss: *Chem. Ing. Tech.*, 2014, vol. 86, pp. 840–47.
10. M. Hillert, B. Sundman, and Z. Wang: *Metall. Trans. B*, 1990, vol. 21B, pp. 303–12.
11. J.E. Saal, D. Shin, A.J. Stevenson, G.L. Messing, and A. Liu: *J. Am. Ceram. Soc.*, 2010, vol. 93 (12), pp. 4158–67.
12. E.M. Levin, C.R. Robbins, H.F. McMurdie, and M.K. Reser: *Phase Diagram For Ceramists*, American ceramic society, Columbus, OH, 1969.
13. W. Wong-Ng, W. Laws, K.R. Talley, Q. Huang, Y. Yan, J. Martin, and J.A. Kaduk: *J. Solid State Chem.*, 2014, vol. 215, pp. 128–34.
14. N.A. Toropov and N.F. Fedorov, Izv. Akad. Nauk SSSR: *Neorg. Mater.*, 1965 vol. 1 [1], pp. 126–130; *Inorg. Mater.* (Engl. Transl.), 1965, vol 1 [1], pp. 110–13.
15. C.M. Jantzen and F.P. Glasser: *Am. Ceram. Soc. Bull.*, 1979, vol. 58 (4), pp. 459–66.
16. M. Zhao, L. Song, and X. Fan: *The Boundary Theory of Phase Diagrams and Its Application*, Springer, Berlin, 2011.
17. J.A. Fahey, W.J. Weber, and F.J. Rotella: *J. Solid State Chem.*, 1985, vol. 60, pp. 145–58.
18. T.H. Le, N.R. Brooks, K. Binnemans, B. Blanpain, M. Guo, and L. Van Meervelt: *Acta crystallogr. E*, 2015, accepted.